Intracluster Anionic Polymerization Initiated by Electron Attachment onto Olefin Clusters $(CH_2{=}CXCN)_N$ (X = Cl, H, D, and CH_3) and $(CH_2{=}CHC_6H_5)_N$

Tatsuya Tsukuda† and Tamotsu Kondow*

Contribution from the Department of Chemistry, School of Science, The University of Tokyo, Bunkyo-ku, Tokyo 113, Japan

Received February 28, 1994®

Abstract: Anionic reactions in the gas-phase clusters of olefin molecules followed by collisional electron transfer from a high-Rydberg krypton atom, Kr**, were investigated systematically by use of mass spectrometry. The olefin molecules used in the present study are 2-chloroacrylonitrile (CAN), acrylonitrile (AN), acrylonitrile-d_1 (AN-d_1), methacrylonitrile (MAN), and styrene (ST). The results are enumerated as follows: (1) Negative ion mass spectra for all the compounds except for styrene exhibit nonstoichiometric mass peaks assigned to $[(CAN)_n - mHCl]^{\bullet-}$, $[(AN)_n - Y]^{\bullet-}$ (Y = H, H_2, HCN, and H_2 + HCN), and $[(MAN)_n - HCN]^{\bullet-}$ which are formed by liberating neutral species, such as HCl, Y, and HCN, from the corresponding intact anions. (2) Elimination of the neutral species was observed only in the cluster anions with $n \geq 2$. (3) Intensity enhancement at $n = 3$ was observed in the intensity distributions of the product anions from the clusters of CAN, AN, and MAN. (4) The elimination reaction proceeded more extensively in a cluster composed of molecules having a more electronegative substituent group. These results show that intracluster anionic polymerization is initiated by electron attachment, and the elimination reaction follows. The trimeric species are produced preferentially as a consequence of formation of a cyclic molecular anion in the cluster and subsequent evaporation of unreacted monomers. A hydrogen-bonded cyclic structure is proposed for a neutral trimer in order to explain the preferential cyclization reaction within the cluster anion.

(I) Introduction

Studies of chemical reactions in molecular clusters provide a rapidly developing area of cluster chemistry.[1-15] With the use of a spatial arrangement of the constituent molecules bound by anisotropic interactions, a chemical reaction can be probed while controlling the parameters of an entrance channel of the reaction, i.e., relative orientation, alignments, and velocity of reactants. This class of intracluster reactions, termed *precursor-geometry-limited (PGL)* reactions, offers a novel means to investigate regiospecific effects on the dynamics of the chemical reactions.[4-7] Recently, collisional activation of a trapped S_N2 reaction intermediate was carried out,[8-10] and the results demonstrate the effects of initial arrangements of the reagents on S_N2 reaction efficiency. In some intracluster ion–molecule reactions, novel ionic products have been observed, having no counterpart in gas-phase bimolecular reactions.[11-16] These reactions might best be described in terms of *termolecular* ion–molecule reactions occurring within the confined media of the clusters.

An *ionic polymerization reaction*[17] in molecular clusters is a typical example of these intracluster ion–molecule reactions and was pursued by several groups recently.[18-31] These results help in the understanding of a wide range of phenomena, such as generation of large molecules in the interstellar space, soot formation in hydrocarbon flames, and the polymerization reactions in the liquid phase. The ionic polymerization reaction proceeds in a more simplified and specified environment than in the condensed phase because of a limited number of reactants involved: in addition, the reaction environment is free of counterion influence. Garvey *et al.* have reported intensity

† Present address: Department of Chemistry, College of Arts and Sciences, The University of Tokyo, Komaba, Meguro, Tokyo 153, Japan.

® Abstract published in *Advance ACS Abstracts*, September 15, 1994.

(1) Wei, S.; Tzeng, W. B.; Castleman, A. W., Jr. *J. Phys. Chem.* **1991**, *95*, 5080–5085.
(2) Papanikolas, J. M.; Gord, J. R.; Levinger, N. E.; Ray, D.; Vorsa, V.; Lineberger, W. C. *J. Phys. Chem.* **1991**, *95*, 8028–8040.
(3) Brutschy, B. *J. Phys. Chem.* **1990**, *94*, 8637–8647.
(4) Jouvet, C.; Boivineau, M.; Duval, M.; Soep, B. *J. Phys. Chem.* **1987**, *91*, 5416–5422.
(5) Wittig, C.; Sharpe, S.; Beaudet, R. A. *Acc. Chem. Res.* **1988**, *21*, 341–347.
(6) Honma, K.; Fujimura, Y.; Kajimoto, O.; Inoue, G. *J. Chem. Phys.* **1988**, *88*, 4739–4747.
(7) Loison, J. C.; Dedonder-Lardeux, C.; Jouvet, C.; Solgadi, D. *J. Phys. Chem.* **1991**, *95*, 9192–9196.
(8) Graul, S. T.; Bowers, M. T. *J. Am. Chem. Soc.* **1991**, *113*, 9696–9697.
(9) Cyr, D. M.; Posey, L. A.; Bishea, G. A.; Han, C.-C.; Johnson, M. A. *J. Am. Chem. Soc.* **1991**, *113*, 9697–9699.
(10) Wilbur, J. L.; Brauman, J. I. *J. Am. Chem. Soc.* **1991**, *113*, 9699–9701.
(11) Shinohara, H.; Sato, H.; Washida, N. *J. Phys. Chem.* **1990**, *94*, 6718–6723.
(12) Garvey, J. F.; Peifer, W.; Coolbaugh, M. T. *Acc. Chem. Res.* **1991**, *24*, 48–54.
(13) King, D. L.; Dixon, D. A.; Herschbach, D. R. *J. Am. Chem. Soc.* **1974**, *96*, 3328–3330.
(14) Behrens, R. B., Jr.; Freedman, A.; Herm, R. R.; Parr, T. P. *J. Chem. Phys.* **1975**, *63*, 4622–4631.
(15) Nieman, J.; Na'aman, R. *Chem. Phys.* **1984**, *90*, 407–416.
(16) Whetten, R. L.; Cox, D. M.; Trevor, D. J.; Kaldor, A. *Surf. Sci.* **1985**, *156*, 8–35.
(17) The intracluster chemical reactions reported in refs 18–31 would be better categorized into *oligomerization reactions* as low molecular weight products are formed by the intracluster chemical reactions. Here, we define the consecutive addition reaction observed within the clusters as *polymerization* in a wider sense.
(18) Morita, H.; Freitas, J. E.; El-Sayed, M. A. *J. Phys. Chem.* **1991**, *95*, 1664–1667.
(19) Garvey, J. F.; Bernstein, R. B. *Chem. Phys. Lett.* **1986**, *126*, 394–398.
(20) Coolbaugh, M. T.; Vaidyanathan, G.; Peifer, W. R.; Garvey, J. F. *J. Phys. Chem.* **1991**, *95*, 8337–8343.
(21) Whitney, S. G.; Coolbaugh, M. T.; Vaidyanathan, G.; Garvey, J. F. *J. Phys. Chem.* **1991**, *95*, 9625–9627.
(22) Coolbaugh, M. T.; Garvey, J. F. *Chem. Soc. Rev.* **1992**, *21*, 163–169.
(23) Coolbaugh, M. T.; Whitney, S. G.; Vaidyanathan, G.; Garvey, J. F. *J. Phys. Chem.* **1992**, *96*, 9139–9144.
(24) El-Shall, M. S.; Marks, C. *J. Phys. Chem.* **1991**, *95*, 4932–4935.
(25) El-Shall, M. S.; Schriver, K. E. *J. Chem. Phys.* **1991**, *95*, 3001–3004.
(26) Feinberg, T. N.; Baer, T.; Duffy, L. M. *J. Phys. Chem.* **1992**, *96*, 9162–9168.
(27) Booze, J. A.; Baer, T. *J. Chem. Phys.* **1992**, *98*, 186–200.
(28) Tsukuda, T.; Kondow, T. *J. Chem. Phys.* **1991**, *95*, 6989–6992.
(29) Tsukuda, T.; Kondow, T. *J. Phys. Chem.* **1992**, *96*, 5671–5673.
(30) Tsukuda, T.; Terasaki, A.; Kondow, T.; Scarton, M. G.; Dessent, C. E.; Bishea, G. A.; Johnson, M. A. *Chem. Phys. Lett.* **1993**, *201*, 351–356.
(31) Tsukuda, T.; Kondow, T. *Chem. Phys. Lett.* **1992**, *197*, 438–442.

0002-7863/94/1516-9555$04.50/0

enhancements (magic numbers) in intensity distributions of $(CH_2{=}R)_n^{\bullet+}$ (R = CH_2, CF_2, and $CHCH_3$) produced by electron impact ionization of $(CH_2{=}R)_N$. The intensity enhancements have been explained in terms of formation of covalently bonded cyclic molecular ions via consecutive addition (polymerization) reactions along with evaporation of unreacted monomers.[19-23] Cationic polymerization reactions which involve sequential elimination of neutral species[32] have been observed in cluster cations of vinyl chloride and isoprene by El-Shall *et al.*[24,25] On the other hand, we have first observed anionic polymerization in clusters of acrylonitrile (AN) by electron attachment and have suggested that an initial orientation of the constituent AN molecules held together by anisotropic hydrogen bonds influences the dynamics of the intracluster anionic polymerization.[28] A similar anionic polymerization and sequential elimination of HCl have been observed in electron attachment onto clusters of 2-chloroacrylonitrile (CAN).[29] In a photodissociation study on dimeric anions, $[(CAN)_2 - m\mathrm{HCl}]^{\bullet-}$ (m = 0–2), the elimination of one HCl molecule is the dominant channel.[30] In the electron attachment to clusters of methyl acrylate (MA), the intensity of $(MA)_5^{\bullet-}$ is enhanced at a higher stagnation pressure and explained by chemical-bond formation in the cluster anion; i.e., intracluster anionic polymerization occurs in $(MA)_5^{\bullet-}$.[31] These mass spectroscopic studies on the intracluster ionic polymerization reactions have suggested that (i) the formation of stable ions leads to the termination of the chain-propagation sequence of the polymerization and (ii) the evaporation of unreacted monomers and/or the elimination of neutral species are the main relaxation pathways for producing the nascent polymeric ions in the gas phase.

This paper presents the experimental results of mass spectroscopic studies on the anionic polymerization in clusters composed of various olefin molecules which include 2-chloroacrylonitrile (CAN, $CH_2{=}CCl(CN)$), acrylonitrile (AN, $CH_2{=}CHCN$), deuterated acrylonitrile (AN-d_1, $CH_2{=}CDCN$), methacrylonitrile (MAN, $CH_2{=}CCH_3(CN)$), and styrene (ST, $CH_2{=}CH\text{-}C_6H_5$). These olefin molecules containing electron-withdrawing groups, such as –CN and $-C_6H_5$, are ready to be polymerized by addition of electrons to them in the condensed phase.[33,34] For example, electrolytic polymerization of an olefin molecule, $CH_2{=}CX(CN)$, is initiated by direct electron addition to it:[33,34]

$$CH_2{=}CX(CN) \xrightarrow{e^-} \underset{\mathbf{1}}{CH_2{=}CX(CN)^{\bullet-}} \qquad (1)$$

The radical anion **1** formed by the electron attachment starts to propagate as

$$\underset{\mathbf{1}}{CH_2{=}CX(CN)^{\bullet-}} \xrightarrow{M} {}^{\bullet}CH_2CX(CN)CH_2C^-X(CN) \xrightarrow{M} \text{larger polymers} \qquad (2)$$

where M represents one of the olefin molecules. The resultant-polymer is known as a "living polymer" which can further react with additional molecules. An olefin molecule having a smaller reduction potential is more reactive in the anionic polymerization.[33,34] If the electron attachment to a cluster of the olefin molecule initiates the anionic polymerization within the cluster in a similar scheme, a large amount of excess energy must be deposited in the nascent polymeric anion because of the high exothermicity of the polymerization reaction. Various relaxation processes would subsequently (or concurrently) occur, such as evaporation of unreacted constituent molecules and/or disruption of chemical bonds in the polymeric anion, so that occurrence of the intracluster anionic polymerization is recognizable through observation of extensive evaporation and/or fragmentation with the use of mass spectrometry.[18-31] The outermost electron of a high-Rydberg krypton atom, $Kr^{**}(n)$ (n = 25–40), was collisionally transferred to the cluster having a positive electron affinity;[35] the kinetic energy of the electron is in the range of 10–20 meV.[36] This ionization method is appropriate for the present study for the following reasons: First, more complex dissociation channels[37,38] are suppressed because the Rydberg electron carries a much smaller amount of kinetic energy than slow electrons from an ordinary electron gun. The suppression of the complex dissociation channels facilitates the analysis of the mass spectra so as to obtain information on the intracluster anionic polymerization reactions from them. Second, the cross section for the attachment of the very slow Rydberg electron onto the clusters is significantly large.[35,39]

The main goal of the present study is to elucidate the fundamental features of the mechanism of the anionic polymerization in an aggregated system composed of a limited number of reactants. In the system, a geometrical arrangement of the reactants should greatly influence the dynamics of the intracluster polymerization as the chain propagation and termination in the polymerization vary critically with the spatial position of its propagating end and that of an adjacent monomer. In fact, polymerization in the crystal of cyclic monomers, such as trioxane, diketene, and β-propiolactone, results in formation of highly ordered polymer products whose structures are affected by the initial arrangements of these monomers in the crystals.[33] On the other hand, no such effect is observed in the anionic oligomerization in the gas phase.[40-44] In an olefin cluster, $(CH_2{=}CX\text{-}CN)_N$, the constituent molecules are considered to constitute a specific geometrical structure because of the anisotropic hydrogen bonding among them, as evidenced in neutral trimers of 1-cyano-4-methylnaphthalene,[45] 1-cyanonaphthalene,[46] and acetonitrile,[47] which have a cyclic geometry. This geometrical structure of the cluster is specifically different from that in the crystal because of its limited number of constituent molecules.[48] The present results demonstrate that a new class of polymeric anions can be synthesized by anionic polymerization in the olefin clusters.

(II) Experimental Section

The experimental apparatus has been described in detail previously,[35] and only a brief description relevant to the present study is given here. The apparatus consists of a cluster beam source, a triple-grid ion source where neutral clusters are ionized, a quadrupole mass filter with an anion

(32) It is often the case that a polymerization reaction which involves elimination of neutral species is termed *condensation polymerization*. However, the elimination reaction observed in the present study is essentially different from the elimination of the neutral species observed in the condensation polymerization, because the present elimination reaction does not proceed stoichiometrically but does sequentially in the course of the degradation of the nascent polymer. Therefore, we classify the intracluster addition–elimination reaction as the polymerization reaction rather than the condensation reaction.

(33) Allcock, H. R.; Lampe, F. W. *Contemporary Polymer Chemistry*; Prentice-Hall: Englewood Cliffs, NJ, 1990; pp 67–120.
(34) Odian, G. *Principles of Polymerization*; Wiley-Interscience: New York, 1991; pp 356–451.
(35) Kondow, T. *J. Phys. Chem.* **1987**, *91*, 1307–1316.
(36) Gallagher, T. F. In *Rydberg States of Atoms and Molecules*; Stebbings, R. F., Dunning, F. B., Eds.; Cambridge University Press: Cambridge, U.K., 1983; p 165.
(37) Tsuda, S.; Yokohata, A.; Umaba, T. *Bull. Chem. Soc. Jpn.* **1973**, *46*, 2273–2277.
(38) Heni, M.; Illenberger, E. *Int. J. Mass. Spectrom. Ion Processes* **1986**, *73*, 127–144.
(39) Knapp, M.; Echt, O.; Kreisle, D.; Recknagel, E. *J. Chem. Phys.* **1986**, *85*, 634–636.
(40) McDonald, R. N.; Chowdhury, A. K.; Setser, D. W. *J. Am. Chem. Soc.* **1980**, *102*, 6491–6498.
(41) McDonald, R. N.; Chowdhury, A. K. *J. Am. Chem. Soc.* **1982**, *104*, 2675–2676.
(42) McDonald, R. N.; Chowdhury, A. K. *J. Am. Chem. Soc.* **1983**, *105*, 2194–2203.
(43) McDonald, R. N.; Chowdhury, A. K. *J. Am. Chem. Soc.* **1985**, *107*, 4123–4128.
(44) Shiga, T.; Yamaoka, H. *Bull. Chem. Soc. Jpn.* **1972**, *45*, 2065–2069.
(45) Ebata, T.; Ito, M.; Itoh, M. *J. Phys. Chem.* **1991**, *95*, 1143–1147.
(46) Itoh, M.; Takamatsu, M.; Kizu, N.; Fujiwara, Y. *J. Phys. Chem.* **1991**, *95*, 9682–9687.
(47) Wright, D.; El-Shall, M. S. *J. Chem. Phys.* **1994**, *100*, 3791–3802.
(48) van de Waal, B. J. *J. Chem. Phys.* **1983**, *79*, 3948–3961.

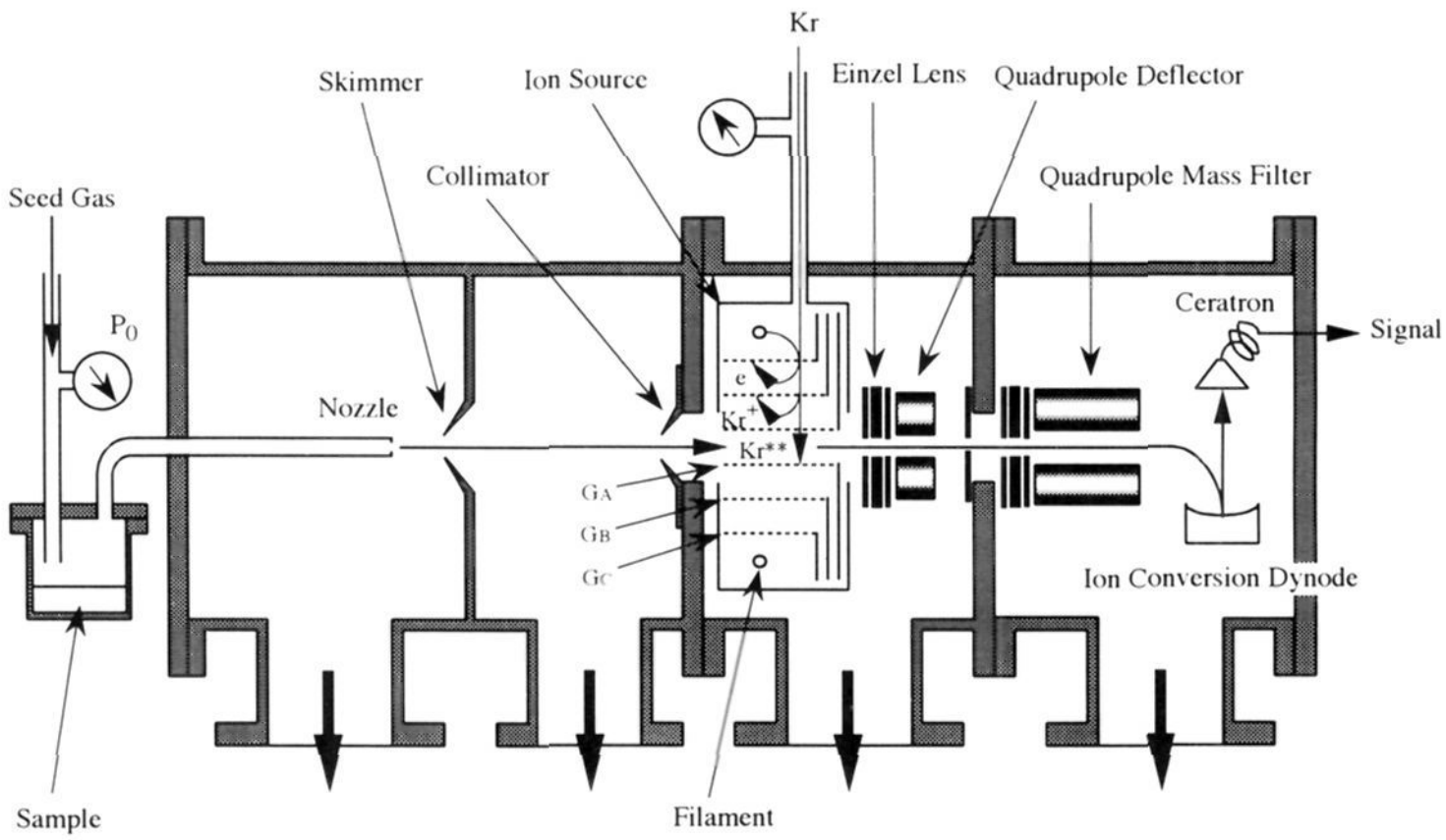

Figure 1. A schematic diagram of the apparatus composed of four vacuum chambers which are differentially pumped. A sample gas was expanded from the nozzle. A supersonic cluster beam was extracted through the skimmer and the collimator. Cluster anions produced in the concentric triple-grid ion source were focused by ion lenses and mass analyzed by the quadrupole mass spectrometer. The cluster anions were converted to positive ions by the ion conversion dynode and detected by the Ceratron electron multiplier.

detector, and a CAMAC system based on an NEC personal computer as shown in Figure 1.

The beam source consists of a sonic nozzle having a platinum aperture of 50 μm in diameter and a conical skimmer with a 310 μm diameter. The nozzle was adjusted externally in three dimensions so as to maximize the total intensity of the product anions. The olefin molecules except for AN-d_1 (CH_2=CDCN) were all commercially available and used without further purification. The deuterated sample, AN-d_1, was prepared by a base-catalyzed exchange with D_2O.[49] The isotopic purity of AN-d_1 thus prepared was estimated to be about 95% by mass spectrometry (15 eV, EI).[37] The sample liquids were degassed and transferred to a reservoir made of stainless steel by freeze–pump–thaw cycles immediately before use. A mixture of He or Ar gas with a sample vapor was prepared by passing He or Ar gas at a stagnation pressure, P_0, of 1.0–5.0 atm over the liquid sample in the reservoir kept at 70 °C. The mixture was expanded through the nozzle into a beam expansion chamber, and a cluster beam of the sample was produced. After being skimmed and collimated, the clusters were introduced into an ionization chamber, where the ion source was mounted. The ion source consists of three concentric cylindrical grids, outside of which filaments are mounted. All these grids and filaments are mounted inside a housing made of stainless steel. Grids G_A, G_B, and G_C are made of stainless-steel mesh with a transmittance of 80%. Four pieces of helical filaments made of a thoriated tungsten wire of 0.15 mm diameter form a regular square. The cluster beam passing through the central region was ionized by impact of either (A) high-Rydberg krypton atoms, Kr**, or (B) free electrons.

(A) Rydberg Atom Impact (RAI). Krypton gas with 99.95% purity was admitted to the ion source at a pushing pressure of typically 0.2 Torr. In the RAI experiment, the pressure of the ionization chamber with a base pressure of (4–5) $\times 10^{-7}$ Torr was maintained at 3×10^{-5} Torr. The Kr atoms were excited by impact of 50 eV electrons in the exterior of G_B. The typical filament current and voltage were 4–5 A and 10–12 V, respectively. Ionic species and electrons were retarded by application of appropriate potentials to the three grids so that only neutral species including Kr** were allowed to enter the central region. Typical voltages applied were –15, –85, –25, and –75 V for G_A, G_B, G_C, and the filaments, respectively. The principal quantum numbers, n, of Kr** were estimated to be in the range of 25–40; Kr** atoms with $n > 40$ were ionized by a static electric field of 140 V/cm applied between G_A and G_B, and Kr** atoms with $n < 25$ could not reach the central region because of their short radiative lifetimes. As described in detail elsewhere,[35] the anionic species were produced by transfer of the Rydberg electrons to the neutral clusters at a single collision condition at this pressure range.

(49) Leitch, L. C. *Can. J. Chem.* **1957**, *35*, 345–347.

(B) Electron Impact (EI). In the EI experiment, electrons emitted from the filaments were accelerated by the three concentric grids into the central region, where the cluster beam was bombarded by the electrons. The average electron energy, $\bar{\epsilon}$, was estimated from the difference between the potential of G_A and that of the filaments. The energy spread (fwhm) was estimated to be about 1 eV at $\bar{\epsilon} \approx 0$ eV by comparison with the measured excitation function for the $SF_6 + e^- \rightarrow SF_6^{\bullet -}$ process.[50]

The anionic species thus produced were focused by einzel lenses and extracted through an entrance slit into the quadrupole mass spectrometer (Extrel, 162-8) installed in a detection chamber. The mass-selected ions were detected by a Ceratron (Murata, EMS-1081B) equipped with an ion conversion dynode made of stainless steel. The mass-to-charge ratios (m/z) of the product anions were calibrated against those of the cluster anions $(CO_2)_n^{\bullet -}$ detected under the same experimental conditions. The transmission and detection efficiencies of the mass spectrometer were not calibrated. The signals from the detector were preamplified (ORTEC, 9301) and registered in a multichannel scaler (Lecroy, 3521A) based on the personal computer. The intensity of an anion with a given m/z value was determined by the area of the corresponding peak in the mass spectrum. Fluctuation of the signal intensity was less than 10% during each experimental run.

(III) Results

(A) Anionic Species Produced by RAI and Their Intensity Distributions. (1) CAN Clusters. Figure 2a shows a typical mass spectrum of the anionic species produced by RAI from the $(CAN)_N$ beam seeded in 5.0 atm of He. A portion of the mass spectrum is expanded in Figure 2b. The mass spectra exhibit fragment anions, $[(CAN)_n - m\text{HCl}]^{\bullet -}$ ($n \geq 2$) and $[\text{Cl}(CAN)_n]^-$ ($n \geq 1$), as well as intact anions, $(CAN)_n^{\bullet -}$, where $[(CAN)_n - m\text{HCl}]^{\bullet -}$ is made by eliminating mHCl from $(CAN)_n^{\bullet -}$. No monomeric anion, $[(CAN)_1 - \text{HCl}]^{\bullet -}$, is observed in the mass spectrum (see Figure 2b). The assignments of the mass peaks are supported by the isotopic pattern of ^{35}Cl and ^{37}Cl.

In Figure 3, the intensities of $[(CAN)_n - m\text{HCl}]^{\bullet -}$ are shown by three-dimensional histograms against m and n. The intensities of $[\text{Cl}(CAN)_n]^-$ are also plotted as a function of n in Figure 3. The intensity of each anionic species is represented by the total area of the mass peaks of the corresponding isotopic species containing ^{35}Cl and ^{37}Cl. The intensity distribution of $(CAN)_n^{\bullet -}$

(50) Christophorou, L. G.; McCorkle, D. L.; Carter, J. G. *J. Chem. Phys.* **1971**, *54*, 253–260.

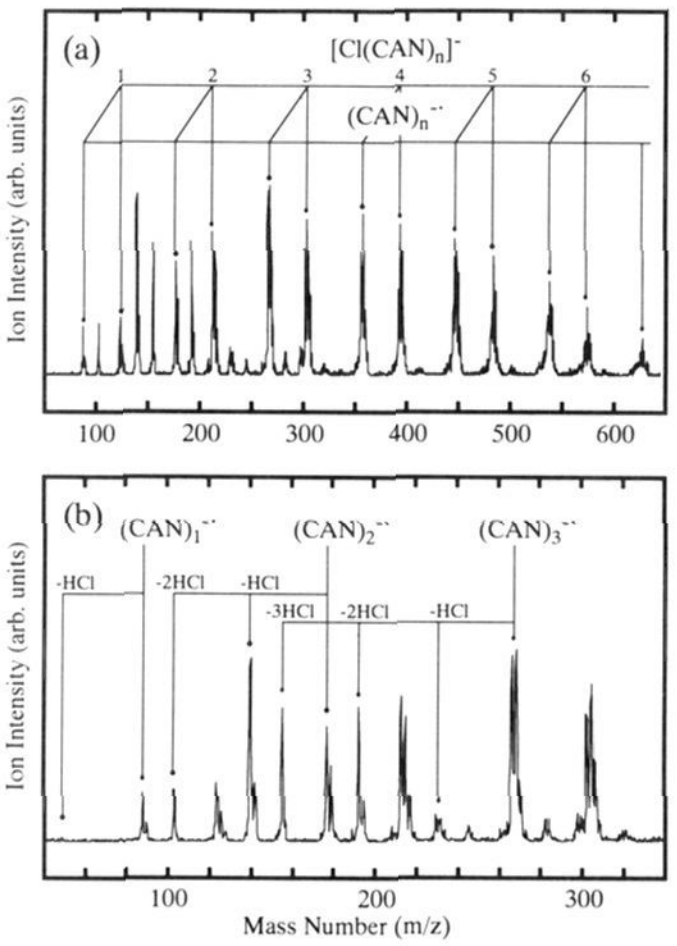

Figure 2. Mass spectra of the anionic species produced from $(CAN)_N$ by RAI: $P_0(He)$ = 5.0 atm. Panel a represents the mass spectrum in the range of m/z = 50–650, while a portion of the mass spectrum is expanded in panel b. Splitting of the mass peaks is due to the isotopic abundance of ^{35}Cl and ^{37}Cl.

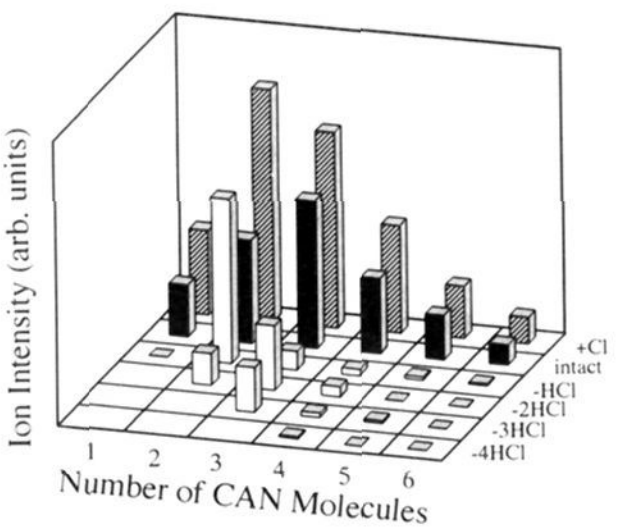

Figure 3. Three-dimensional histograms of peak intensities of the anionic species produced from $(CAN)_N$ by RAI: $P_0(He)$ = 5.0 atm. The intensities of $(CAN)_n^{\bullet-}$ and $[(CAN)_n - mHCl]^{\bullet-}$ are plotted as a function of the number of CAN molecules, n, and that of HCl molecules eliminated, m. The intensities of $[Cl(CAN)_n]^-$ are plotted in the column denoted +Cl as a function of n.

exhibits the most prominent peak at n = 3 as shown in Figure 3. The fragment anions $[(CAN)_n - mHCl]^{\bullet-}$ with n = 2 and 3 are abundant while those with $n \geq 4$ are scarcely populated.

(2) AN Clusters. Figure 4 shows a typical mass spectrum of the anionic species produced by RAI from the $(AN)_N$ beam seeded in 4.0 atm of He. Various fragment anions along with intact anions, $(AN)_n^{\bullet-}$ ($n \geq 1$), are discernible in the mass spectrum, especially in the mass regions in the vicinity of $(AN)_3^{\bullet-}$ and $(AN)_6^{\bullet-}$ (see Figure 4). These fragment anions are assigned to trimeric and hexameric anions of AN which liberate neutral species with m/z 1, 2, 27, and 29 (see section IVB). Figure 5 shows a portion of a mass spectrum of the anionic species produced by RAI from the $(AN\text{-}d_1)_N$ beam seeded in 4.0 atm of He. In addition to an intact anion, $(AN\text{-}d_1)_3^{\bullet-}$, trimeric anions in which neutral species with m/z 2, 4, 27, and 31 are removed from $(AN\text{-}d_1)_3^{\bullet-}$ are observed. These observations lead us to conclude that the trimeric anions are best described as $[(AN)_3 - H]^-$, $[(AN)_3 - H_2]^{\bullet-}$, $[(AN)_3 - HCN]^{\bullet-}$, and $[(AN)_3 - HCN - H_2]^{\bullet-}$,

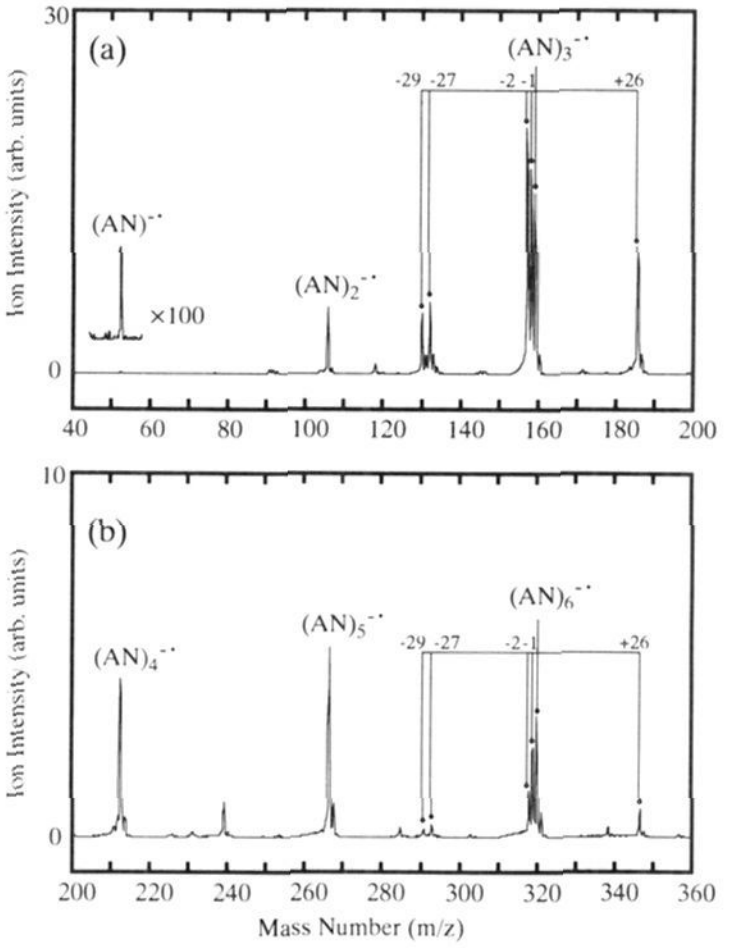

Figure 4. Mass spectra of the anionic species produced from $(AN)_N$ by RAI: $P_0(He)$ = 4.0 atm. Panels a and b show the mass spectra of $(AN)_n^{\bullet-}$ with n = 1–3 and n = 4–6, respectively, where the ordinate of panel b is scaled up by a factor of 3 compared to that of panel a. The fragment species whose m/z values are smaller than that of $(AN)_n^{\bullet-}$ by 1, 2, 27, and 29 are assigned to $[(AN)_n - Y]^{\bullet-}$ (Y = H, H_2, HCN, and H_2 + HCN), respectively. The anions $[(AN)_n - Y]^{\bullet-}$ (Y = H, H_2, HCN, and H_2 + HCN) exhibit extraordinarily high abundances at n = 3 and 6. The mass peak whose m/z value is larger than that of $(AN)_3^{\bullet-}$ by 26 is attributed to a mixture of $[CN(AN)_3]^-$ and $[(AN)_4 - HCN]^{\bullet-}$.

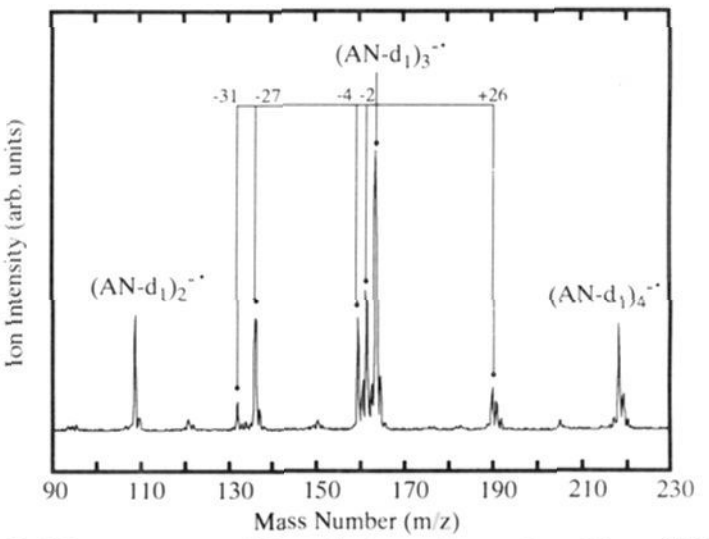

Figure 5. Mass spectrum of the anionic species produced from $(AN\text{-}d_1)_N$ by RAI: $P_0(He)$ = 4.0 atm. The fragment species whose m/z values are smaller than that of $(AN\text{-}d_1)_3^{\bullet-}$ by 2, 4, 27, and 31 are assigned to $[(AN\text{-}d_1)_3 - Y]^{\bullet-}$ (Y = D, D_2, HCN, and D_2 + HCN), respectively.

respectively. These anions are hereafter simplified as $[(AN)_3 - Y]^{\bullet-}$ (Y = H, H_2, HCN, and H_2 + HCN). Anionic species, such as $[(AN\text{-}d_1)_3 - D_2]^{\bullet-}$ and $[(AN\text{-}d_1)_3 - D_2 - HCN]^{\bullet-}$ (or $[(AN\text{-}d_1)_3 - DH - DCN]^{\bullet-}$), are observed in which two deuterium atoms originally bonded to different constituent AN-d_1 molecules are liberated as a molecule. Figure 5 shows that the mass peak whose m/z value is larger than that of $(AN)_3^{\bullet-}$ by 26 (see Figure 4) is attributed to two species, $[CN(AN)_3]^-$ and $[(AN)_4 - HCN]^{\bullet-}$. It is also shown that the anion whose m/z value is larger than that of $(AN)_n^{\bullet-}$ by 1 should be assigned to $(AN)_n^{\bullet-}$ containing one ^{13}C atom rather than $[H(AN)_n]^-$.[28]

Parts a–e of Figure 6 display the intensity distributions of $(AN)_n^{\bullet-}$ and $[(AN)_n - Y]^{\bullet-}$ (Y = H, H_2, HCN, and H_2 + HCN) as a function of the number of AN molecules in the anions, respectively. The fragment anions, $[(AN)_n - Y]^{\bullet-}$ (Y = H, H_2,

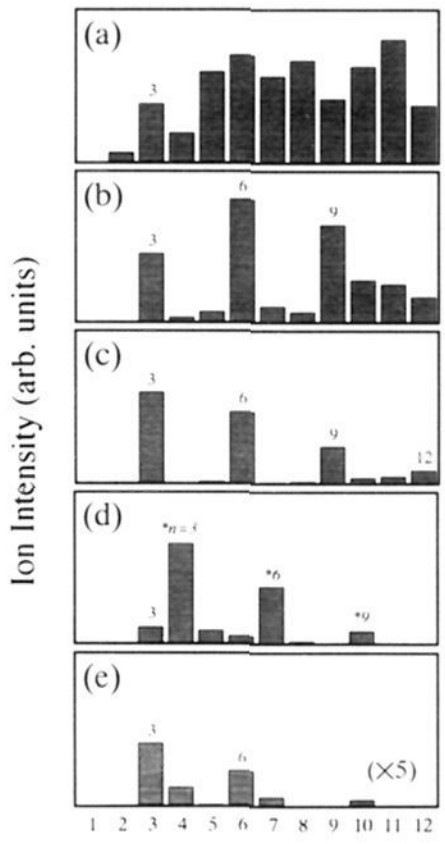

Figure 6. Intensity distributions of the anionic species produced from $(AN)_N$ by RAI: $P_0(He)$ = 4.0 atm. The intensities of (a) $(AN)_n^{\bullet-}$, (b) $[(AN)_n - H]^-$, (c) $[(AN)_n - H_2]^{\bullet-}$, (d) $[(AN)_n - HCN]^{\bullet-}$, and (e) $[(AN)_n - H_2 - HCN]^{\bullet-}$ are plotted as a function of the number of AN molecules, n. The intensity enhancements in the intensity distribution of $[(AN)_n - HCN]^{\bullet-}$ at n = 4, 7, and 10 are attributed to the peaks associated with $[CN(AN)_n]^-$ (n = 3, 6, and 9), which overlap with the $[(AN)_n - HCN]^{\bullet-}$ (n = 4, 7, and 10) peaks. These overlapping peaks are indicated by asterisks.

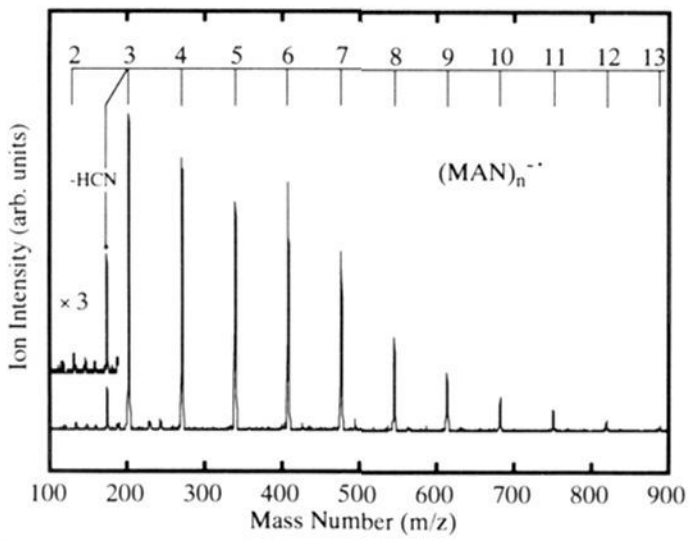

Figure 7. Mass spectrum of the anionic species produced from $(MAN)_N$ by RAI: $P_0(He)$ = 5.0 atm. The anions assigned to $(MAN)_n^{\bullet-}$ and $[(MAN)_n - HCN]^{\bullet-}$ have large populations at n = 3.

and H_2 + HCN), with n = 3, 6, 9, ..., are extraordinarily abundant in the intensity distributions. The intensity distributions of $(AN)_n^{\bullet-}$ and $[(AN)_n - HCN]^{\bullet-}$ also exhibit significant enhancements at n = 3. The intensity enhancements in the intensity distribution of $[(AN)_n - HCN]^{\bullet-}$ at n = 4, 7, and 10 are attributed to the peaks associated with $[CN(AN)_n]^-$ (n = 3, 6, and 9), which overlap with the $[(AN)_n - HCN]^{\bullet-}$ (n = 4, 7, and 10) peaks at the present mass resolution. These overlapping peaks are indicated by the asterisks in Figure 6d.

(3) MAN and ST Clusters. Figures 7 and 8 represent mass spectra of the anionic species generated by RAI from the $(MAN)_N$ and $(ST)_N$ beams seeded in 5.0 atm of He, respectively. For $(MAN)_N$, fragment anions, $[(MAN)_n - HCN]^{\bullet-}$ ($n \geq 3$), are observed along with intact anions, $(MAN)_n^{\bullet-}$ ($n \geq 2$). The trimeric anions $(MAN)_3^{\bullet-}$ and $[(MAN)_3 - HCN]^{\bullet-}$ are highly populated in the intensity distribution as shown in Figure 7. In contrast, for $(ST)_N$, only intact anions, $(ST)_n^{\bullet-}$ ($n \geq 3$), are observed and

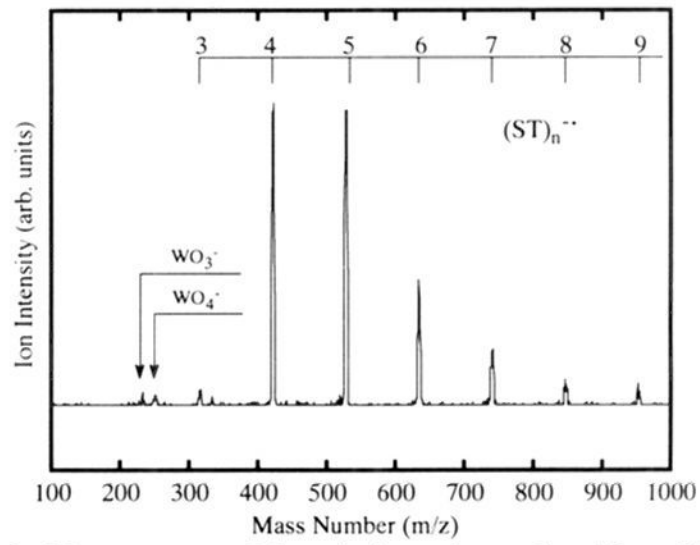

Figure 8. Mass spectrum of the anionic species produced from $(ST)_N$ by RAI: $P_0(He)$ = 5.0 atm.

Table 1. Summary of the Observed Anions, Threshold Sizes (n_{th}), Magic Numbers (n_{mgc}), and Reduction Potentials of the Olefin Monomers

olefin monomers	observed anions	n_{th}	n_{mgc}	–reduction potential[a] (V)
CAN	$(CAN)_n^{\bullet-}$	1	3	<2.09[b]
	$[(CAN)_n - mHCl]^{\bullet-}$	2	3	
	$[Cl(CAN)_n]^-$	1		
AN	$(AN)_n^{\bullet-}$	1	3	2.09
	$[(AN)_n - H]^-$	2	3, 6, 9	
	$[(AN)_n - H_2]^{\bullet-}$	2	3, 6, 9	
	$[(AN)_n - H_2 - HCN]^{\bullet-}$	3	3, 6	
MAN	$(MAN)_n^{\bullet-}$	2	3	3.13
	$[(MAN)_n - HCN]^{\bullet-}$	3	3	
ST	$(ST)_n^{\bullet-}$	3		3.19

[a] From ref 51. [b] Because of the higher electronegativity of Cl than that of H, the reduction potential of CAN should be smaller than that of AN.

form a smooth intensity distribution at every stagnation pressure of 1.0–5.0 atm measured (see Figure 8).

Table 1 lists n_{th} and n_{mgc} of all the anionic species produced by RAI, where n_{th} represents the threshold size below which no product anion is observed and n_{mgc} represents the size at which the ion intensity is particularly large. The reduction potential of each olefin molecule which gives a measure of its reactivity of the anionic polymerization[51] is also listed in Table 1. The essential features derived from Table 1 are enumerated as follows: (1) Fragment cluster anions have threshold sizes larger than 2. No monomeric fragment anions are detected in the RAI of the olefin clusters. (2) The intensity distributions of both the intact and the fragment anionic products from $(CAN)_N$, $(AN)_N$, and $(MAN)_N$ exhibit intensity enhancements at n = 3. (3) The threshold size for the formation of $(M)_n^{\bullet-}$ increases as the reduction potential of the constituent molecule, M, increases. (4) The elimination reaction proceeds more extensively in the cluster anions composed of molecules with a lower reduction potential.

(B) Dependences of Intensity Distributions on the Stagnation Pressure and/or Seed Gas. Peak intensities of the trimeric anions were significantly enhanced in the intensity distributions of the anionic products from $(CAN)_N$ and $(AN)_N$ (see Table 1). In order to identify neutral precursors of these trimeric anions, the ion intensities were measured as a function of the stagnation pressure, P_0, or the intensity distributions were measured with the use of different seed gases. Larger clusters are produced more favorably when (1) the sample vapor is seeded in Ar rather than in He and (2) P_0 increases.[52,53]

(51) Yamazaki, N.; Tanaka, I.; Nakahama, S. *J. Macromol. Sci., Chem.* **1968**, *A2*, 1121–1137.
(52) Grover, T. R.; Herron, W. J.; Coolbaugh, M. T.; Peifer, W. R.; Garvey, J. F. *J. Phys. Chem.* **1991**, *95*, 6473–6481.
(53) Walters, E. A.; Grover, T. R.; Clay, J. T.; Cid-Aguero, P.; Willcox, M. V. *J. Phys. Chem.* **1992**, *96*, 7236–7243.

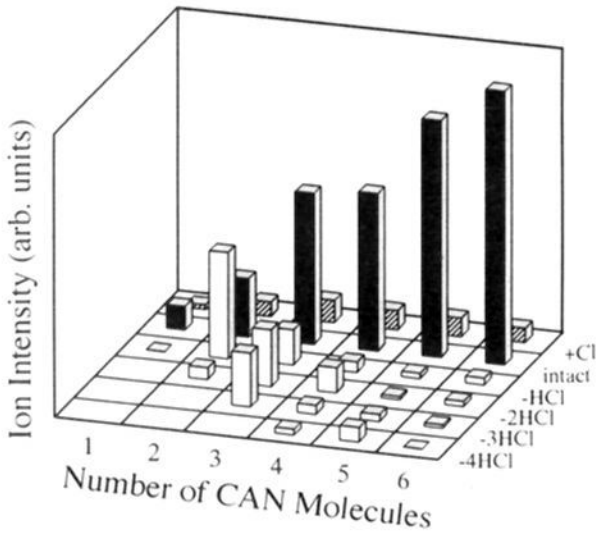

Figure 9. Three-dimensional histograms of the peak intensities of the anionic species produced from $(CAN)_N$ by RAI: $P_0(Ar) = 5.0$ atm.

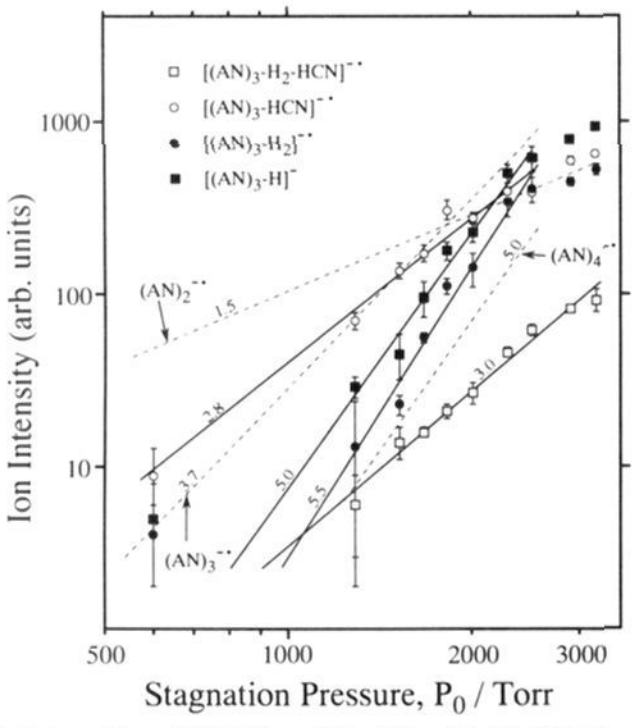

Figure 10. Intensities of $[(AN)_3 - Y]^{\bullet-}$ (Y = H, H_2, HCN, and H_2 + HCN) and $(AN)_n^{\bullet-}$ with $n = 2$–4 as a function of the stagnation pressure of helium, $P_0(He)$. The intensities of each species are fit to P_0^{α}, and the value of α obtained by the least-squares method is presented on each curve.

(1) CAN Clusters. Figure 9 represents the intensity distribution of the anionic products generated from the $(CAN)_N$ beam seeded in 5.0 atm of Ar. Comparison of Figure 9 with Figure 3 shows that the intensity ratio $[(CAN)_n - mHCl]^{\bullet-}/(CAN)_n^{\bullet-}$ does not change with n, even though $(CAN)_n^{\bullet-}$ anions with larger sizes are generated more favorably by using Ar as a seed gas. This result implies that $[(CAN)_n - mHCl]^{\bullet-}$ is produced from the same precursor as $(CAN)_n^{\bullet-}$ by liberation of HCl molecules. The peak intensities of $(CAN)_3^{\bullet-}$ and $[(CAN)_3 - mHCl]^{\bullet-}$ are enhanced more distinctly in Ar seed than in He seed. This result leads us to conclude that $(CAN)_3^{\bullet-}$ and $[(CAN)_3 - mHCl]^{\bullet-}$ are formed upon electron attachment onto $(CAN)_N$ with $N \geq 3$. The intensities of $[Cl(CAN)_n]^-$ are greatly suppressed when Ar is used as the seed gas.

(2) AN Clusters. The intensities of $(AN)_n^{\bullet-}$ (n = 2–4) and $[(AN)_3 - Y]^{\bullet-}$ (Y = H, H_2, HCN, and H_2 + HCN) produced by RAI are plotted against the stagnation pressure of He, P_0(He), in Figure 10. The intensities vary in proportion to $P_0(He)^{\alpha}$ in the onset pressure region (scaling law); a similar behavior has been reported for various van der Waals clusters.[52,53] The α values obtained by the least-squares method are shown on each curve in Figure 10. Significantly steeper slopes of the curves for $(AN)_3^{\bullet-}$ and $[(AN)_3 - Y]^{\bullet-}$ (Y = H, H_2, and H_2 + HCN) than that for $[(AN)_3 - HCN]^{\bullet-}$ indicate that $(AN)_3^{\bullet-}$ and $[(AN)_3 - Y]^{\bullet-}$ (Y = H, H_2, and H_2 + HCN) are produced from parent clusters larger than those of $[(AN)_3 - HCN]^{\bullet-}$. The dependence of the mass spectrum on the seed gas (He or Ar) used lends further support for this interpretation. Figure 11 shows the mass spectra of the anionic species produced from $(AN)_N$, which is generated by expansion of the AN sample seeded in 4.0 atm of He or Ar. The intensity ratios $(AN)_3^{\bullet-}/[(AN)_3 - HCN]^{\bullet-}$ and $[(AN)_3 - Y]^{\bullet-}/[(AN)_3 - HCN]^{\bullet-}$ (Y = H, H_2, and H_2 + HCN) are larger when $(AN)_N$ with larger sizes is more abundant in the beam. It follows from this finding that $(AN)_3^{\bullet-}$ and $[(AN)_3 - Y]^{\bullet-}$ (Y = H, H_2, and H_2 + HCN) are generated from $(AN)_N$ ($N \geq 3$) by electron attachment along with subsequent evaporation of AN monomers.

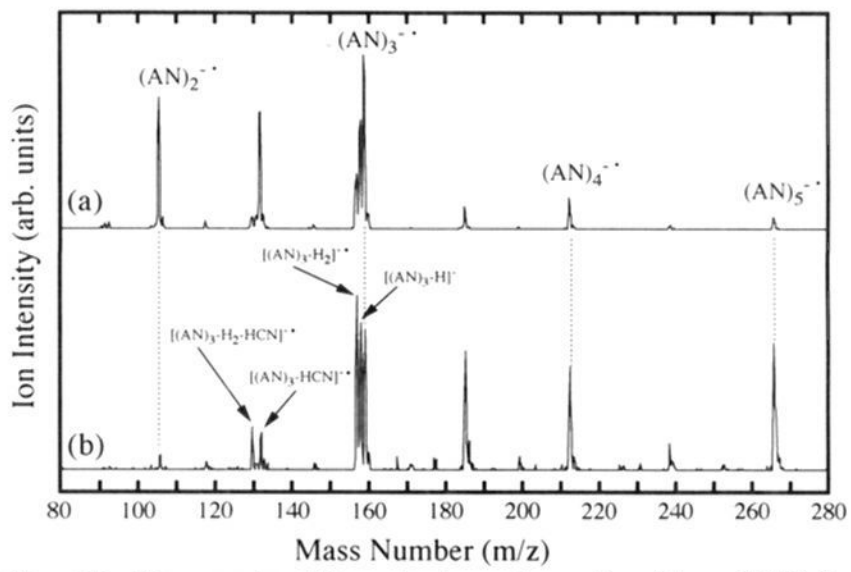

Figure 11. Mass spectra of the anionic species produced from $(AN)_N$ by RAI: (a) $P_0(He) = 4.0$ atm; (b) $P_0(Ar) = 4.0$ atm.

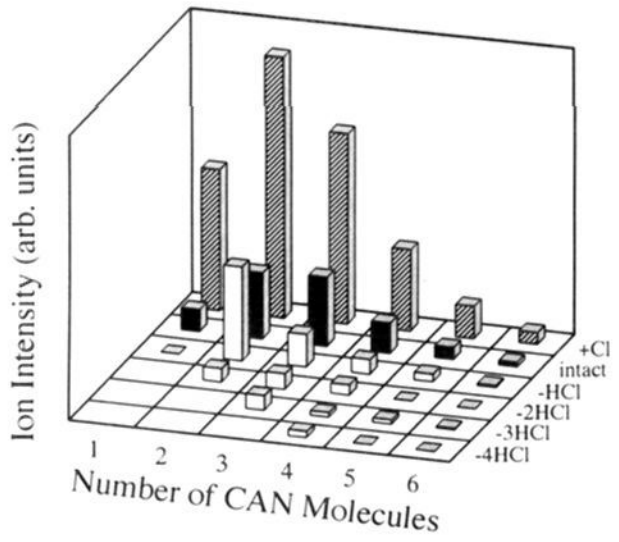

Figure 12. Three-dimensional histogram of the peak intensities of the anionic species produced from $(CAN)_N$ by EI ($\bar{\epsilon} = 6$ eV): $P_0(He) = 5.0$ atm.

(C) Dependences of Intensity Distributions on Electron Energy. Nascent cluster anions formed by attachment of energetic electrons undergo extensive evaporation and/or dissociation since a lot of energy is introduced. The intensity distributions of the anionic products from $(CAN)_N$ and $(AN)_N$ were measured at different impact energies of electrons, $\bar{\epsilon}$.

(1) CAN Clusters. Figure 12 shows the intensity distribution of the anionic species produced by EI ($\bar{\epsilon} = 6$ eV) from the $(CAN)_N$ beam seeded in 5.0 atm of He. The intensity distributions of $(CAN)_n^{\bullet-}$ and $[(CAN)_n - mHCl]^{\bullet-}$ with respect to n do not change appreciably with the electron impact energy in the energy range up to 6 eV (see Figures 3 and 12). In contrast, the relative intensity of $[(CAN)_n - mHCl]^{\bullet-}$ with respect to $(CAN)_n^{\bullet-}$ increases with an increase in the electron impact energy; e.g., the intensity ratio $[(CAN)_3 - HCl]^{\bullet-}/(CAN)_3^{\bullet-}$ is larger with EI than RAI. These findings imply that the excess energy deposited in the CAN cluster anions is consumed dominantly through liberation of HCl but not through evaporation of CAN monomers. In order to liberate HCl, a chemical bond should be formed between the constituent monomers. It is also found in the EI experiment that the monomeric fragment anion $[(CAN)_1 - HCl]^{\bullet-}$ is not detected, while elimination of one Cl atom from $CAN^{\bullet-}$ occurs as a minor channel. This result indicates that $[(CAN)_n - HCl]^{\bullet-}$ is not

formed via dissociative electron attachment to one of the CAN molecules in $(CAN)_N$. The anions $[(Cl(CAN)_n]^-$ become more abundant as the kinetic energy of the incoming electron increases to 6 eV.

(2) AN Clusters. Figure 13 shows the intensity distribution of the anionic species produced by EI ($\bar{\epsilon}$ = 8 eV) from the $(AN)_N$ beam seeded in 4.0 atm of He. All the trimeric species, $[(AN)_3 - Y]^{\bullet -}$, become more abundant whereas those of $n \neq 3k$ remain scarcely populated, as the energy of the incoming electron increases. The relative intensities of $[(AN)_3 - Y]^{\bullet -}$ (Y = H, H_2, HCN, and H_2 + HCN) produced by RAI and EI are almost the same. These features can be explained in such a manner that three AN monomers evaporate concurrently when more energy is introduced by the incoming electron. The anionic species with $n < 3$ are not populated any more, even at the impact energy of 8 eV, probably because the constituent molecules in the trimeric anions are bound together with a strong chemical bond.

(IV) Discussion

(A) Anionic Polymerization in $(CAN)_N$ Initiated by Electron Attachment. The following arguments show that electron attachment to $(CAN)_N$ intiates intracluster anionic polymerization and that the fragment anions $[(CAN)_n - m\text{HCl}]^{\bullet -}$ are produced as a result. As shown in Figure 3, the elimination reaction proceeds in a nascent cluster anion composed of more than two CAN molecules, and in some cases, several HCl molecules are released from the nascent anion. These experimental findings imply that at least two CAN molecules are involved in the HCl elimination reaction. The energetics of the elimination reaction supports the inference that HCl molecules are released as a result of the intracluster anionic polymerization. For simplicity, the heat of reaction for $(CAN)_2 + Kr^{**} \rightarrow [(CAN)_2 - HCl]^{\bullet -} + HCl + Kr^+$ is estimated by assuming the following three routes:

$$[CH_2{=}CCl(CN)\cdots CH_2{=}CCl(CN)] + Kr^{**} \rightarrow [CH{\equiv}C(CN)^{\bullet -}\cdots CH_2{=}CCl(CN)] + HCl + Kr^+ \quad (3A)$$

$$\rightarrow [CH_2{=}C^-(CN)\cdots {}^{\bullet}CH{=}CCl(CN)] + HCl + Kr^+ \quad (3B)$$

$$\rightarrow [CH_2{=}C(CN){-}CH{=}CCl(CN)]^{\bullet -} + HCl + Kr^+ \quad (3C)$$

where HCl is removed from one and two constituents in $(CAN)_2$ in reactions 3A and 3B, respectively, without any further reactions between the resultant species. In reaction 3C, two species, $CH_2{=}C^-(CN)$ and $^{\bullet}CH{=}CCl(CN)$, react to form a new C—C bonding between them. The heats of reaction for reactions 3A–3C are given by

$$\Delta H_{rxn}(3A) \approx D(CH_2C(CN){-}Cl) + D(H{-}CHCCl(CN)) - D(H{-}Cl) - \Delta E - EA_a(CH{\equiv}C(CN)) \quad (4A)$$

$$\Delta H_{rxn}(3B) \approx D(CH_2C(CN){-}Cl) + D(H{-}CHCCl(CN)) - D(H{-}Cl) - EA_a(CH_2{=}C^{\bullet}(CN)) \quad (4B)$$

$$\Delta H_{rxn}(3C) \approx D(CH_2C(CN){-}Cl) + D(H{-}CHCCl(CN)) - D(H{-}Cl) - D(CH_2C(CN){-}CHCCl(CN)) - EA_a(H_2C{=}C(CN){-}CH{=}CCl(CN)) \quad (4C)$$

The bond dissociation energy of H—Cl, D(H—Cl), is reported to be 4.4 eV.[54] The bond dissociation energies $D(CH_2C(CN){-}Cl)$, $D(H{-}CHCCl(CN))$, and $D(CH_2C(CN){-}CHCCl(CN))$ are approximated by those of $CH_2CH{-}Cl$ (3.9 eV),[55] $H{-}CHCH_2$ (4.7 eV),[56] and $CH_2CH{-}CHCH_2$ (4.9 eV),[57] respectively. The term ΔE represents an energy gain by formation of a triple bond from the double bond and is estimated to be 2.5 eV from the difference in the dissociation energies of CH≡CH and $CH_2{=}CH_2$. The adiabatic electron affinities of CH≡C-(CN) and $CH_2{=}C^{\bullet}(CN)$ are calculated to be 0.2 eV[58] and 1.5 eV,[59] respectively. The adiabatic electron affinity of $H_2C{=}C(CN){-}CH{=}CCl(CN)$ cannot be evaluated but must be a positive quantity.[60] In the estimation, the ionization potential of Kr** (10–20 meV)[36] is neglected and the binding energies of $(CAN)_2$ and the anionic complexes are assumed to be unchanged throughout the processes of reactions 3A–3C. The heats of reaction for reactions 3A–3C turn out to be +1.5, +2.7, and $-(0.7 + EA_a(H_2C{=}C(CN){-}CH{=}CCl(CN)))$ eV, respectively. Reaction 3C is only exothermic among the three reactions, and

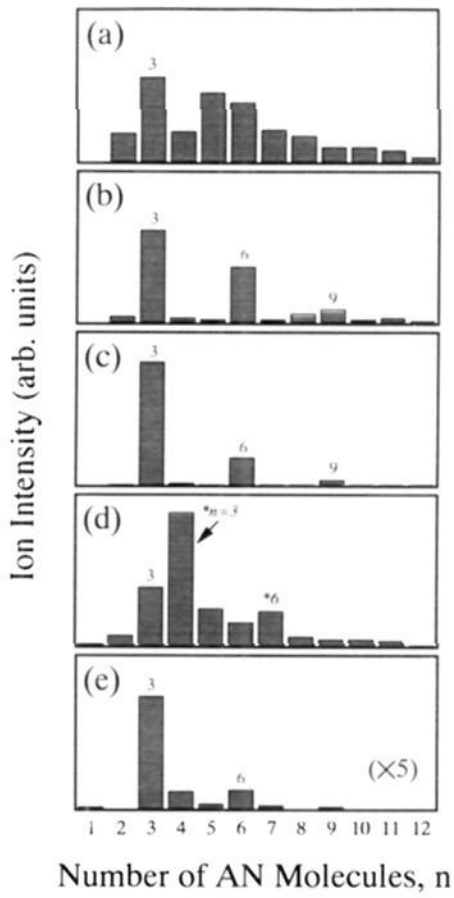

Figure 13. Intensity distributions of the anionic species produced from $(AN)_N$ by EI ($\bar{\epsilon}$ = 8 eV): P_0(He) = 4.0 atm. The intensities of (a) $(AN)_n^{\bullet -}$, (b) $[(AN)_n - H]^-$, (c) $[(AN)_n - H_2]^{\bullet -}$, (d) $[(AN)_n - HCN]^{\bullet -}$, and (e) $[(AN)_n - H_2 - HCN]^{\bullet -}$ are plotted as a function of the number of AN molecules, n.

(54) Darwent, B. de B. Bond Dissociation Energies in Simple Molecules. NSRDS-NBS31; National Bureau of Standards: Washington, DC, 1970.

(55) The bond dissociation energy $D(CH_2C(CN){-}Cl)$ was estimated to be 3.9 eV from the standard enthalpies of formation ΔH(Cl) = 1.3 eV, $\Delta H(CH_2{=}CHCl)$ = 0.4 eV, and $\Delta H(CH_2{=}C^{\bullet}H)$ = 3.0 eV.

(56) Golden, D. M.; Benson, S. W. *Chem. Rev.* **1969**, *69*, 125–134.

(57) The bond dissociation energy $D(CH_2CH{-}CHCH_2)$ was estimated to be 4.9 eV from the standard enthalpies of formation $\Delta H(CH_2CH{-}CHCH_2)$ = 1.14 eV and $\Delta H(CH{=}CH_2)$ = 3.00 eV.

(58) The adiabatic electron affinity (EA_a) of ethylene (–1.55 eV: Burrow, P. D.; Jordan, K. D. *Chem. Phys. Lett.* **1975**, *36*, 594–598) increases by 1.88 eV (Mirek, J.; Buda, A. *Z. Naturforsch.* **1984**, *34a*, 386–390) on the substitution of H for CN. The EA_a of CH≡C(CN) was estimated to be +0.2 eV on the assumption that the EA_a of acetylene (–1.7 eV: Frenking, G. *Chem. Phys. Lett.* **1983**, *100*, 484–487) increases by the same amount.

(59) The adiabatic electron affinity of $CH_2{=}C^{\bullet}(CN)$ is given by the equation $EA_a(CH_2{=}C^{\bullet}(CN)) = D(CH_2{=}C(CN){-}H) - \Delta H_{acid}(AN) + IP(H)$, where the bond dissociation energy $D(CH_2{=}C(CN){-}H)$ is reported to be 4 eV and the acidity of AN, $\Delta H_{acid}(AN)$, is reported to be 16.1 eV. The ionization potential of hydrogen, IP(H), is known to be 13.6 eV. By putting these values all together, the EA_a value turns out to be 1.5 eV.

(60) The molecule $H_2C{=}C(CN)CH{=}CCl(CN)$ has a structure in which a hydrogen atom of $H_2C{=}CCl(CN)$ is replaced by a $H_2C{=}C(CN)$ radical whose electron affinity is positive.[58] Because the electron affinity of $H_2C{=}CCl(CN)$ turns out to be positive from the present study (see Figure 2), the adiabatic electron affinity of $H_2C{=}C(CN)CH{=}CCl(CN)$ must be a positive quantity.

Scheme 1

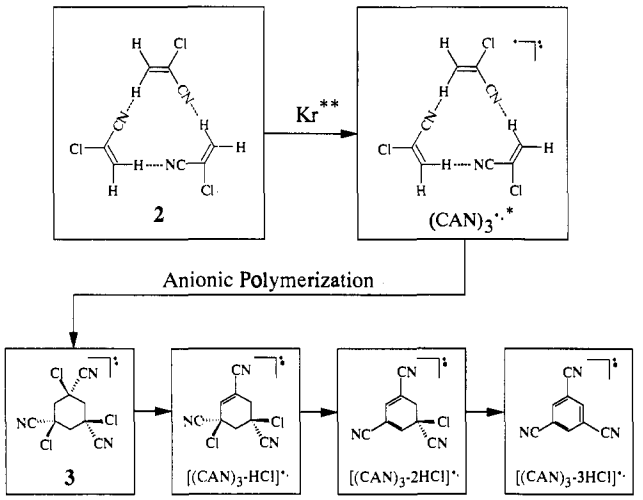

hence is the most likely to proceed in the electron attachment to $(CAN)_2$. The chemical bond formation between the constituent molecules in $[(CAN)_2 - HCl]^{\bullet-}$ is also supported by the finding that CAN molecules do not evaporate extensively even in the electron attachment of a 6 eV electron. Further elimination of one more HCl molecule was observed in $[(CAN)_2 - HCl]^{\bullet-}$ to yield $[(CAN)_2 - 2HCl]^{\bullet-}$ which is likely to have a polyene structure, $[H_2C{=}C(CN)C{\equiv}CC{\equiv}N]^{\bullet-}$.

Similarly, the trimeric species $[(CAN)_3 - mHCl]^{\bullet-}$ (m = 1–3) are considered to be polymeric anions; $[(CAN)_3 - 3HCl]^{\bullet-}$ is identified as a radical anion of 1,3,5-tricyanobenzene (m/z 153) by the photoelectron spectrum of $[(CAN)_3 - 3HCl]^{\bullet-}$ in comparison with that of (1,3,5-tricyanobenzene)$^{\bullet-}$.[61] Evidently, $[(CAN)_3 - 3HCl]^{\bullet-}$ having a six-membered carbon ring is formed by the intracluster trimerization. Naturally, $[(CAN)_3 - HCl]^{\bullet-}$ and $[(CAN)_3 - 2HCl]^{\bullet-}$ are regarded as reaction intermediates for the HCl elimination reaction and also possess cyclic structures. In contrast, $[(CAN)_n - mHCl]^{\bullet-}$ ($n \geq 4$) are scarcely populated in the intensity distribution (see Figure 3) probably because polymeric anions larger than a tetramer are not produced efficiently in the electron attachment onto $(CAN)_N$.

In summary, the electron attachment onto $(CAN)_N$ initiates rearrangement of chemical bonds within the cluster via the eliminative anionic polymerization. When the Rydberg electron (10–20 meV) is transferred to $(CAN)_N$, the electron is captured by a CAN molecule and the intracluster polymerization starts because the excess energy associated with the electron attachment (i.e., the adiabatic electron affinity of $(CAN)_N$) surmounts the activation barrier of the reaction. The reaction energy of the intracluster anionic polymerization causes "heating" of the nascent polymeric anion, and HCl molecules are subsequently liberated so as to release the reaction energy from it. A similar HCl elimination reaction has also been observed when $[(CAN)_2 - mHCl]^{\bullet-}$ (m = 0–2) is excited by a laser irradiation.[30] This sequential elimination of HCl molecules is parallel to that in the thermal degradation of a CAN polymer.[62,63] The efficient formation of $[(CAN)_3 - mHCl]^{\bullet-}$ is explained in terms of a cyclization reaction of $(CAN)_3$ upon electron attachment (see Scheme 1).

The formation of the cyclic molecular anion **3** hinders further chain propagation, and as a result, $[(CAN)_n - mHCl]^{\bullet-}$ ($n \geq 4$) is not formed efficiently (a kinetic bottleneck).[19-23] The kinetic bottleneck due to the cyclization in the very fast intracluster anionic polymerization is attributable to the structure of $(CAN)_3$. The hydrogen-bonded cyclic structure **2** is proposed for $(CAN)_3$ on the basis of the structures of neutral trimers of similar compounds, such as 1-cyano-4-methylnaphthalene,[45] 1-cyanonaphthalene,[46] and acetonitrile:[47] The electronegative CN group and the acidic H atom form a hydrogen bond in a linear configuration which is energetically favorable because the lone pair of the nitrogen extends along the C–N axis. Due to this initial arrangement of three CAN molecules in **2**, the trimeric anions undergo cyclization preferentially to form an internally excited molecular anion, **3**, which is a precursor of $[(CAN)_3 - mHCl]^{\bullet-}$. The efficient production of $[(CAN)_3 - mHCl]^{\bullet-}$ as well as $(CAN)_3^{\bullet-}$ from $(CAN)_N$ ($N > 3$) is expressed as follows (see section IIIB1):

$$(CAN)_N \xrightarrow{Kr^{**}} (CAN)_N^{-\bullet} \quad (5A)$$

$$\rightarrow [(CAN)_3 - mHCl]^{\bullet-} + mHCl + (N-3)CAN \quad (5B)$$

$$\rightarrow (CAN)_3^{\bullet-} + (N-3)CAN \quad (5C)$$

These processes are also attributable to the structure of $(CAN)_N$ in which the trimer unit in the ring geometry **2** is bound weakly by N – 3 CAN monomers. In fact, such a structure has been reported for the tetramer of 1-cyano-4-methylnaphthalene.[45] Upon electron attachment onto $(CAN)_N$, the trimer unit **2** in it undergoes cyclization much faster than further propagation. As a result, the cyclic anion **3** with sufficient internal energy is formed, being stable against further addition of a CAN molecule to it because of a high activation barrier associated with C–C bond breaking. The exothermic reaction energy of the trimerization is released by evaporating unreacted CAN monomers, yielding the trimeric anions of $[(CAN)_3 - mHCl]^{\bullet-}$ and $(CAN)_3^{\bullet-}$ (processes 5B and 5C). Therefore, it is concluded that the cyclic arrangement of three CAN molecules in $(CAN)_N$ is responsible for the efficient termination of the propagation step in the intracluster anionic polymerization.

The mass spectrum exhibits a series of mass peaks assigned to $[Cl(CAN)_n]^-$ with $n \geq 1$ (see Figure 2). However, the chemical composition of $[Cl(CAN)_n]^-$ cannot be identified unambiguously only by the mass spectrum.

(B) Anionic Polymerization in $(AN)_N$ Initiated by Electron Attachment. The anionic products $[(AN)_{3k} - Y]^{\bullet-}$ (Y = H, H_2, HCN, and H_2 + HCN) observed in the present study are assignable to polymeric species for the following reasons: First, the enthalpy change of the reaction for the $[(AN)_1 - Y]^{\bullet-}$ $(AN)_{3k-1}$ formation rules out the possibility of the formation of such cluster anions. It has been reported that electron attachment onto an AN molecule initiates the following reactions:[37,38]

$$AN + e^- \rightarrow \underset{m/z\ 52}{C_3H_2N^-} + H^\bullet \qquad \Delta H \approx 2.5\ eV \quad (6)$$

$$\rightarrow \underset{m/z\ 51}{C_3HN^{-\bullet}} + H_2 \qquad \Delta H \approx 4\ eV \quad (7)$$

$$\rightarrow \underset{m/z\ 26}{CN^-} + C_2H_3^\bullet \qquad \Delta H \approx 1.6\ eV \quad (8)$$

$$\rightarrow \underset{m/z\ 26}{C_2H_2^{-\bullet}} + HCN \qquad \Delta H \approx 3.7\ eV \quad (9)$$

$$\rightarrow \underset{m/z\ 24}{C_2^{-\bullet}} + H_2 + HCN \qquad \Delta H \approx 4.9\ eV \quad (10)$$

These reactions are endothermic even if two more AN molecules participate in these reactions as solvents, since a typical solvation energy of an anionic species by a neutral molecule amounts to about 1 eV at maximum.[64] Therefore, $[(AN)_{3k} - Y]^{\bullet-}$ (Y = H, H_2, HCN, and H_2 + HCN) anions observed in the present study do not have such a structure that the anionic core, $[(AN)_1 - Y]^{\bullet-}$,

(61) Tsukuda, T.; Kondow, T.; Lavrich, D. J.; Cyr, D. M.; Scarton, M. G.; Johnson, M. A. Unpublished results.
(62) Grassie, N.; Grant, E. M. *J. Polym. Sci., C* **1967**, *16*, 591–599.
(63) Hiraoka, H.; Lee, W. *Macromolecules* **1978**, *11*, 622–624.
(64) Keesee, R. G.; Castleman, A. W., Jr. *J. Phys. Chem. Ref. Data* **1986**, *15*, 1011–1071.

is solvated by $3k - 1$ AN monomers. Second, the dependence of the intensity distribution on the electron impact energy supports the formation of chemical bonds between the constituent monomers. The populations of the smaller species than the trimeric species do not increase significantly, even when an excess energy up to 8 eV is introduced (see Figure 13). This finding is compatible with the conjecture that the monomers are bound together with a strong bonding, such as a σ bond. Third, hydrogen atoms originally bonded to different constituent molecules in the clusters are removed (presumably as a hydrogen molecule) in $[(AN)_3 - H_2]^{\bullet-}$ and $[(AN)_3 - H_2 - HCN]^{\bullet-}$. These processes are essentially different from reactions 7 and 10 where hydrogen molecules are removed from one AN molecule. A chemical reaction, such as polymerization, between more than two molecules is involved in the formation of these fragment anions. The elimination reaction of HCN is in direct analogy with the thermal degradation of an AN polymer where HCN loss is a dominant pathway.[65]

Anionic oligomerization of mass-selected nucleophiles (Nu), such as CH_3O^-,[41] $^-CH_2CN$,[41] and $O_2^{\bullet-}$,[43] with AN molecules has been examined by McDonald *et al.* in the gas phase. Their results show that the anionic oligomerization proceeds via 1,4-addition (Michael) of the precursor anion with AN molecules to form a "living" oligomer, $Nu(CH_2CH(CN))_nCH_2C^-H(CN)$. A termination step for the propagation of the anionic oligomerization has been observed at $n = 4$ for CH_3O^-,[41] $n = 3$ for $^-CH_2CN$,[41] and $n = 1$ for $O_2^{\bullet-}$,[43] respectively. Reduction of reactivity toward further addition has been attributed to stabilization of the oligomeric anion through electrostatic interaction or structural change.

In contrast, the propagation step of the anionic polymerization within the AN cluster anions is terminated by preferential cyclization of the trimeric anions. As stated in section IIIB2, $[(AN)_3 - Y]^{\bullet-}$ (Y = H, H_2, HCN, and H_2 + HCN) and $(AN)_3^{\bullet-}$ are produced preferentially from $(AN)_N$ ($N \geq 3$) as follows:

$$(AN)_N \xrightarrow{K^{**}} (AN)_N^{\bullet-} \qquad (11A)$$

$$\rightarrow [(AN)_3 - Y]^{\bullet-} + Y + (N-3)AN \qquad (11B)$$

$$\rightarrow (AN)_3^{\bullet-} + (N-3)AN \qquad (11C)$$

The favorable formation of $[(AN)_3 - Y]^{\bullet-}$ and $(AN)_3^{\bullet-}$ from $(AN)_N$ ($N \geq 3$) is explained by assuming that $(AN)_N$ consists of an AN trimer unit in the ring geometry **4** with additional weakly bound AN monomers. The formation processes of $[(AN)_3 - Y]^{\bullet-}$ from **4** are expressed in Scheme 2 based on the schemes of 1,4-addition[41,43] for the propagation step and of efficient cyclization of the trimeric anions for the termination step. Proposed structures for $[(AN)_3 - Y]^{\bullet-}$ are also represented in Scheme 2. For example, it is evident from Figure 5 that one or two α-hydrogens are removed from the trimeric anion to form $[(AN)_3 - H]^-$ or $[(AN)_3 - H_2]^{\bullet-}$; this result is reasonable because of the high acidity of the α-proton.[66]

The intracluster anionic polymerization takes place and is terminated as a consequence of formation of a cyclic trimeric anion, **5**. The resulting molecular anion **5** is nonreactive against other constituent molecules. Namely, the nascent cluster anion is composed of the cyclic molecular anion **5** and unreacted AN molecules bound together through electrostatic interaction. The excited anion **5** releases the excess energy associated with the trimerization reaction by releasing unreacted molecules within the cluster (process 11C) and various neutral species Y (process 11B). The evaporation of the unreacted AN molecules facilitates the production of $[(AN)_3 - Y]^{\bullet-}$ as well as $(AN)_3^{\bullet-}$, whose intensity is prominent in the intensity distribution of $(AN)_n^{\bullet-}$.

Scheme 2

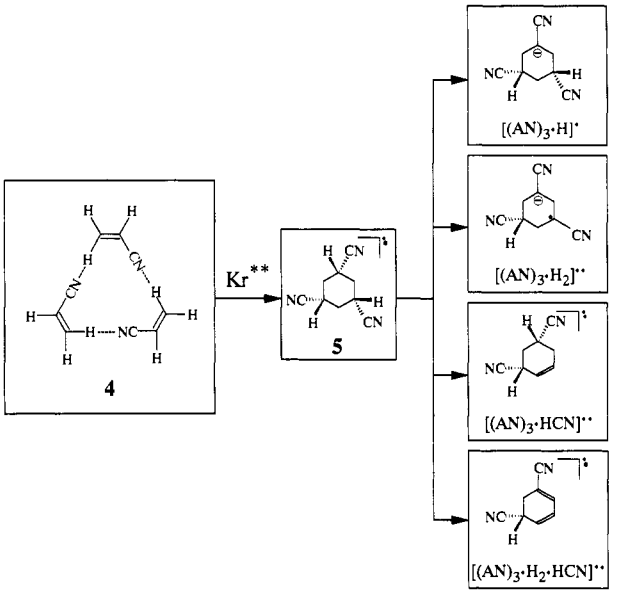

The anions $[(AN)_{3k} - Y]^{\bullet-}$ with $k \geq 2$ do not seem to be cyclic molecular anions made of $3k$ monomers because there is no evidence that $6k$-carbon rings ($k \geq 2$) are particularly stable. As is shown in Figure 13, three AN molecules evaporate concurrently when the excess energy is transmitted from the incoming electron. This result implies that $[(AN)_{3k} - Y]^{\bullet-}$ is composed of the anionic core $[(AN)_3 - Y]^{\bullet-}$ and $k - 1$ AN trimer units stable against fragmentation. As $(AN)_3$ is not particularly stable as is shown in the positive ion mass spectrum of $(AN)_N$,[67] the stable AN trimer units should be held together as a consequence of intermolecular covalent bond formation. It is, thus, possible to explain the formation of $[(AN)_{3k} - Y]^{\bullet-}$ in such a manner that the energy released by the anionic trimerization causes the electron transfer from the nascent trimeric anion $(AN)_3^{\bullet-*}$ to another site in the AN cluster, before its dissociation into $[(AN)_n - Y]^{\bullet-}$. This electron transfer initiates the polymerization reaction in another hydrogen-bonded trimer unit, **4**, and results in formation of another cyclic molecule within one cluster system. In order that another cyclization of the trimeric anions takes place, $(AN)_N$ with $N \geq 6$ should consist of several trimer units, **4**, and monomers weakly bound in the system.

The structure and the reaction scheme of the $[CN(AN)_n]^-$ ($n = 3, 6, 9, \ldots$) formation are unclear: the structure of $[CN(AN)_n]^-$ might be described as either a van der Waals complex of CN^- and AN molecules[66] or a polymerization product formed by nucleophilic addition of CN^- to the β-carbon of an AN molecule followed by sequential addition of other AN molecules.

(C) Anionic Polymerization in $(MAN)_N$ and $(ST)_N$ Initiated by Electron Attachment. Similar arguments on $(MAN)_N$ lead us to conclude that $[(MAN)_3 - HCN]^{\bullet-}$ is a cyclic molecular anion formed via intracluster anionic polymerization: The formation process of $[(MAN)_3 - HCN]^{\bullet-}$ from $(MAN)_3$ upon electron attachment is shown in Scheme 3. In this case, too, the preferential cyclization process of the trimeric anions hinders further reaction. Any decisive evidence was not provided for the anionic polymerization within $(ST)_N$ upon electron attachment.

The strong correlation between the extent of the elimination in a cluster anion and the reactivity of its constituent molecule gives further circumstantial evidence for the occurrence of the anionic polymerization in the CAN, AN, and MAN systems: It has been well established that the olefin molecule having a smaller

(65) Burlant, W. J.; Parsons, J. L. *J. Polym. Sci.* **1956**, *22*, 249–256.
(66) Bernasconi, C. F.; Stronach, M. W.; Depuy, C. H.; Gronert, S. *J. Am. Chem. Soc.* **1990**, *112*, 9044–9052.

(67) The mass spectrum of AN cluster cations formed by EI ($\bar{\epsilon}$ = 70 eV) exhibits a salient series of mass peaks assignable to $(AN)_n^{\bullet+}$ and $H^+(AN)_n$, whose intensity distributions are smooth with respect to n. The experimental finding implies that $(AN)_3$ is not particularly stable and is not abundant in the $(AN)_N$ beam.

Scheme 3

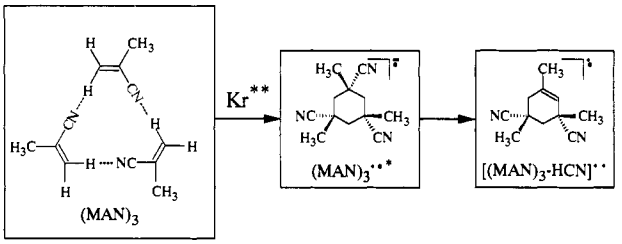

reduction potential exhibits higher reactivity for the anionic polymerization.[33,34] Evidently, the elimination reaction proceeds more extensively in a cluster anion made of an olefin molecule having a smaller reduction potential, i.e., in the order of CAN > AN > MAN > ST (see Table 1 and Figures 2, 4, 7, and 8). This correlation indicates that the elimination observed in the present study is caused by the anionic polymerization.

(V) Concluding Remarks

The conclusions of the present study are summarized as follows: (1) Intracluster anionic polymerization proceeds in $(CAN)_N$, $(AN)_N$, $(AN\text{-}d_1)_N$, and $(MAN)_N$ following electron attachment, and as a result, neutral species are eliminated from the intact anions larger than dimers, in direct analogy with thermal degradation of the corresponding polymers. (2) The trimer anions are particularly abundant because of a kinetic bottleneck in the propagation step so that cyclization of the trimeric anions is favored. (3) The dynamics of the intracluster anionic polymerization is influenced by the initial arrangement of the constituent molecules in $(CH_2{=}CXCN)_N$. A hydrogen-bonded cyclic structure is proposed for $(CH_2{=}CXCN)_3$ so as to explain the preferential formation of the trimeric anions. (4) The fragment anions are produced more efficiently from a given cluster anion when the reactivity for polymerization of the constituent olefin monomer is higher, in the order of CAN > AN > MAN > ST. This trend indicates that the fragmentation is caused by the highly exothermic intracluster anionic polymerization.

Acknowledgment. Professor Kozo Kuchitsu is greatly appreciated for his valuable discussion and critical reading of the paper. The authors are indebted to Professors Takashi Nagata and Renji Okazaki and Dr. Akira Terasaki for their illuminating discussion. Professor Mark A. Johnson is greatly acknowledged for the valuable discussion on the photodissociation and photoelectron studies of the CAN cluster anions. The authors thank Professor Suehiro Iwata and Dr. Tohru Kobayashi for their comments on the structure of the olefin trimers. The synthesis of deuterated acrylonitrile was performed with the help of the members of Professor Koichi Narasaka's laboratory. The authors are grateful to Messrs. Masahiko Ichihashi and Yuuji Fukuda for the discussion on the structure of the AN cluster anions. T.T. is supported by the Fellowships of Japan Society for the Promotion of Science for Japanese Junior Scientists. The present work has been supported by a Grant-in-Aid for Scientific Research on Priority Areas by the Ministry of Education, Science and Culture of Japan.